Refracting saddle wave model of stable fundamental particles

Robert E Galloway
8523 East 9th St., Tulsa, OK 74112
E-mail: regallow@sbcglobal.net

Abstract. This paper presents a semi-classical structural model for electrons, protons, and their antiparticles. The structure is based on refractive interaction of an electromagnetic saddle wave on an elliptic ring path. These elliptical ring particles show a net attractive centripetal force maintaining the closed path, equal but opposite charges in pair production, and spin $h/2\pi$ (with one caveat). A deviation from Coulomb's Law similar in effect to a short-range attractive force is inherent to a ring's electromagnetic field at small distances. The calculated electron magnetic moment anomaly is approximately 0.0055%, about 21 times better fit than the Bohr magneton provides. About 97% of the remaining anomaly could be due to a missing component in the CODATA experimental value. The proton magnetic moment anomaly is only about 0.07% between theory and experiment. Calculated proton rms radius differs significantly from 2002 CODATA R_p, but the author identifies one possible systematic assumption in the analysis of electron scattering data that would account for the entire difference. Hypothesized anomalous dispersion limits the number of stable particle pairs to two (electron-positron and proton-antiproton), determines

their masses, assists in determining refractive indices and phase velocity, and provides additional stability.

PACS: 14.60.Cd, 14.20.-c, 41.20.-q, 12.90.+b

1. Introduction

A successful theory of matter must include a viable explanation for the stability and known properties of the four stable fundamental particles with rest mass, the electron, positron, proton, and antiproton. The Standard Model of physics does so by introducing extremely complicated physical concepts and particle models. This paper presents one structural electromagnetic model for the four stable particles using only pre-Standard Model physics and certain hypotheses. It provides stability, uniqueness of mass, quantized charge and spin, and magnetic moments that account for most of the anomalies between theory and experiment. Along the way, it demonstrates a natural divergence from Coulomb's Law and identifies an electron magnetic moment component that might not be accounted for in existing experiments. And it identifies a possible error in the analysis of experimental proton rms charge radius. Several tests of the model are possible.

2. Generalized model

In electron-positron pair production, one photon of sufficient energy with group wavelength $\lambda_{g\sim}$ and group frequency $\nu_{g\sim}$ interacts with external fields strong enough to divide the photon's energy into halves and create a particle from each half. For this paper's theory, essentially two plane-polarized photons are generated from one, then half-cycles with aligned magnetic field vectors from each photon are combined into particle rings. Figure 1 describes the resulting two

particle rings. This paper does not attempt to model the pair production process, but rather the resulting particles. The same structural model is found to apply equally well to protons and antiprotons.

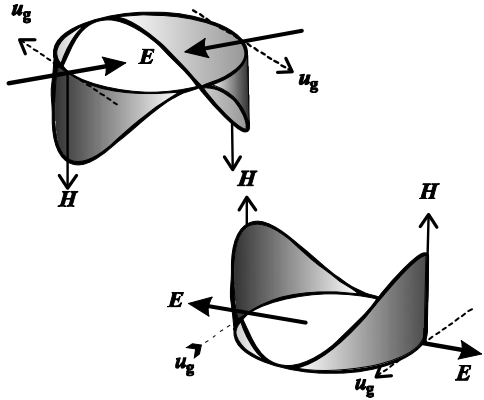

Fig. 1. Ring particles from pair production

2.1. Hypothesized requirements

The hypotheses used by this theory to generate any pair of stable rest mass particles from a photon are:

- Two photon half-cycles with aligned magnetic field vectors associate as one particle ring. This provides a balanced saddle wave configuration and generates oppositely charged particle rings.
- Electromagnetic interaction across the diameter generates a refractive index. The refractive index is key to the particle ring's size, stability, and properties.

The hypothesis that limits the number of stable rest mass pairs to two, specifies their masses, helps determine phase contributions to particle properties, and improves stability is:

- One anomalous dispersion wavelength exists for the ring particle electromagnetic waves.

The hypotheses necessary to nearly match experimental magnetic moments for the electron and proton are:

- Both group and phase wave components of the energy contribute to magnetic moment.
- A non-integer index of refraction causes precession, as long as the particle is otherwise stable.

2.2. General model structure

Consider either particle ring in Figure 1. At any point on the circumference, the EM field extending from the opposite diameter has an opposing Poynting vector. The opposing EM field creates a refractive index *n* that varies around the ring in proportion to its field strength. Varying as a sine function, *n* refracts the wave, changing its group and phase wavelengths and generating an elliptical path with $\lambda_{g\sim}/n = \pi r$. The sine variation of *n* increases the radius to $2r/\sqrt{2}$ at maximum and decreases it to $\sqrt{2}r/2$ at minimum, where *r* is a circular radius that would result if the energy were evenly distributed. The majority of this paper's analysis uses a circular ring instead of an ellipse for simplicity. The values of *n* derived later for electron and proton appear to be averages for their rings, inherently including adjustments for the difference in perimeter of an ellipse versus a circle and relativistic effects, because neither type of adjustment was found to improve accuracy.

A ring's energy has group wavelength $\lambda_g = 2\lambda_{g\sim} = 2\pi r n$ and group frequency $\nu_g = \nu_{g\sim}/2$, giving the particle half the energy of the originating photon. The particle's group wavelength and frequency then give

$$\lambda_g \nu_g = c = 2\pi r n \nu_g , \tag{1}$$

where *c* is the velocity of light in free space. The saddle wave has the same group and phase properties of an equivalent photon. Both group and phase components are important in this model.

2.3. Anomalous dispersion effects

Anomalous dispersion is evident for all substances [2 p. 470], so considering the possibility in EM interactions is appropriate. For anomalous dispersion to occur, there must exist the equivalent of an absorption wavelength. The author hypothesizes that there exists one unique photon wavelength λ_1 in the interval defined by one-half the equivalent energy wavelength of a proton and an electron. For that wavelength, refractive index $n=1$, $dn/d\lambda$ is very large or undefined, and the equivalent of an absorption band exists.

Figure 2 is a proposed anomalous dispersion diagram for this model. At minimum and maximum n, $dn/d\lambda_g = 0$. The velocity of light, group velocity u_g, refractive index, and group wavelength in free space relate through the equation [2 p. 478]

$$\frac{c}{u_g} = n - \frac{dn}{d\lambda_g}.$$

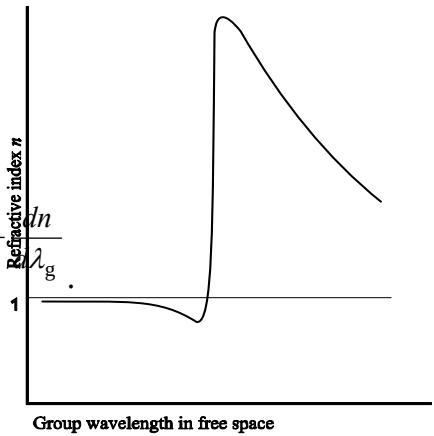

Fig. 2. Representative anomalous dispersion curve

For dispersive media (refractive index varies with wavelength or frequency), the following relationship between group and phase velocities holds [4]:

$$u_g u_\phi = c^2.$$

Then when $dn/d\lambda_g=0$ at minimum and maximum n in Figure 2,

$$u_g = \frac{c}{n}, \qquad (2)$$

$$u_\phi = nc\,. \tag{3}$$

The "absorption" wavelength between minimum and maximum *n* for which $n=1$ is λ_1. Through one absorption wavelength, two energy levels are allowed for pair production. The wavelength at maximum *n* is the electron-positron pair generating wavelength, and the wavelength at minimum *n* is the proton-antiproton pair generating wavelength. Specific *n* values for the two energies will be determined later.

Stability of a ring structure at $dn/d\lambda_g = 0$ is enhanced by the anomalous behavior of *n*. The value of $\lambda_g = 2\pi rn$ or $\lambda_{g\sim} = \pi rn$ cannot change without changing the energy of a ring particle, so the product of *r* and *n* is constant. Consider the curve in Figure 2 at maximum *n* for a particle of radius *r*. A reduction in *r* (move left on the curve from maximum *n*) results in a decrease of *n*, and *r* is forced back to a larger value. The particle is not allowed to implode. Attempt to increase *r*, and n decreases at a slower rate than the increase in *r*. As a result, the refractive index is higher than allowed for the increased *r*, and *r* is reduced until stability is restored. Similar reasoning applies to the proton-antiproton associated wavelength at minimum *n*, with modification due to the inverted *n* curve. Assume the proton is stable at minimum *n*. Decrease *r*, and *n* increases but at a rate slower than the decrease in *r*, driving *r* back to its larger stable value. Increase *r*, and *n* increases instead of decreasing, driving *r* down until stability is restored.

The anomalous dispersion hypothesis may apply only to the specific EM interaction in these ring particles or it may apply in general to all photons in an imposed EM field. If it applies to all photons *and* if refractive index $n<1$ for all wavelengths shorter than λ_1, a modification of existing EM theory would be appropriate. In

that case, the group - phase relationship of photons would swap at λ_1. For wavelengths greater than λ_1, a quantum is defined by group wavelength λ_g, group velocity $u_g \le c$, phase velocity $u_\phi \ge c$, phase wavelength $\lambda_\phi \le \lambda_g$, and energy transport is at group velocity u_g. These relationships reflect standard EM theory. At wavelengths shorter than λ_1 the group - phase relationship would swap, with a quantum defined by phase wavelength λ_ϕ, phase velocity $u_\phi \le c$, group velocity $u_g \ge c$, group wavelength $\lambda_g \le \lambda_\phi$, and energy transport at the velocity u_ϕ (assuming the names group and phase aren't simply swapped). Superluminal energy transport velocities would still be still forbidden at all wavelengths by stipulating that energy transport occurs at the lower of group and phase velocities. The best group - phase wavelength relationship that fits this paper's theory is for phase wavelength $\lambda_\phi = \lambda_g / n$. Using (1), that leads to $\lambda_\phi = 2\pi r$ which would assist in particle stability (ie phase wavelength is an integer multiple of $2\pi r$, corresponding to a similar quantum requirement for electron orbits in the Bohr hydrogen atomic model) and would further support the analysis of spin later in Section 5.

2.4. Mapping EM energy to the structure

A cross-section of the average electric field for a photon's half-cycle is described in Figure 3. The equations shown were derived using Coulomb's Law and determining a set of derivatives that result in E when integrated over their included distances.

$$E = \frac{kq}{r^2} = \int_{-\infty}^{0} \frac{-kq}{2r(x-r)^2}\,dx + \int_{0}^{\infty} \frac{-kq}{2r(x+r)^2}\,dx\,,$$

where $k = (4\pi\varepsilon_0)^{-1}$ and ε_0 is the universal electric constant.

The energy distribution of a photon is then inversely proportional to distance from the propagation axis (perpendicular to the paper at origin 0,0). Offset distance r prevents E from going to infinity at the propagation axis and is inversely proportional to the energy of the photon. Charge q is a point charge equivalent that electric field E represents.

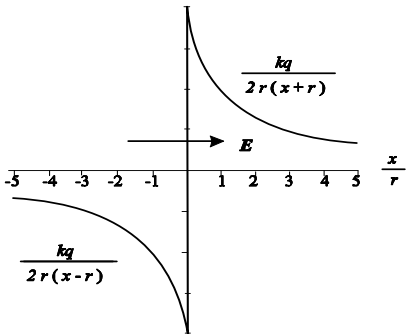

Fig. 3. Photon half-cycle ***E*** cross-section, $k = (4\pi\varepsilon_0)^{-1}$

By placing mirror images of this field onto opposing sides of a circle, Figure 4 shows a cross-section of the interacting E fields of a negative charge ring particle. A positive charge particle would show the fields swapped. $\boldsymbol{E_1}$ and $\boldsymbol{E_2}$ are associated with the bold half-cycle at $x/r = -1$, while $\boldsymbol{E_3}$ and $\boldsymbol{E_4}$ are associated with the dashed half-cycle at $x/r = 1$. Figure 5 shows the resulting approximate net value E_{NET} in

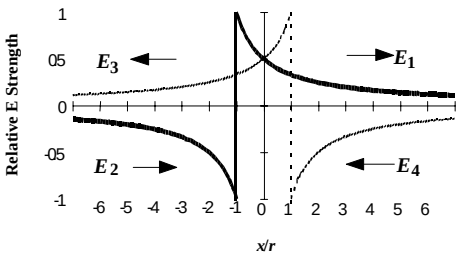

Fig. 4. Photon field ***E*** mapped to electron ring

cross-section. The shape of this curve is in general agreement with experimental evidence of the potential well of antiprotons or protons.

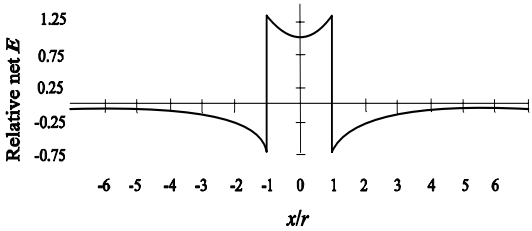

Fig. 5. Representative cross-section of electron E_{NET}

Electrons and positrons are not currently thought to have an internal structure, but this model predicts one. For all calculated properties, including the reported proton experimental radius, the electron's structure has significant importance.

3. Balance of forces

Relative to an external frame of reference at rest, a wave of EM energy circulates on the ring perimeter. A net centripetal force acting inward is necessary to maintain a closed orbit.

3.1. Electrostatic force

Total electrostatic force across the ring structure is equal to the product of net charge and net *E* at the diameter. Referring to Figure 3, the following equations give cross-section *E* component values for a negative charge ring. For the purpose of these equations, equal distribution of energy around the ring rather than sinusoidal makes calculations simpler. The index of refraction, also not included, is the number of times a group wave of specified energy would wrap around the circumference if $n=1$. These equations include summing over *n* circumference wraps of the particle's energy wavelength.

$$E_1 = \frac{kq}{2r(2r+x)}, \quad x > -r, \tag{4}$$

$$E_2 = \frac{kq}{2rx}, \quad x \le -r\,, \tag{5}$$

$$E_3 = \frac{kq}{2r(2r-x)}, \quad x < r\,, \tag{6}$$

$$E_4 = \frac{-kq}{2rx}, \quad x \ge r\,. \tag{7}$$

The net electric field at any point is the sum of fields present at that point. Inside the diameter, $\boldsymbol{E_1}$ and $\boldsymbol{E_3}$ combine to form $\boldsymbol{E_{NET}}$. Outside the right diameter, $\boldsymbol{E_1}$ and $\boldsymbol{E_4}$ combine into $\boldsymbol{E_{NET}}$ as seen from other particles.

$$E_{\mathrm{NET}} = \frac{2kq}{\left(4r^2 - x^2\right)}, \quad -r < x < r \quad \text{(inside the diameter).} \tag{8}$$

$$E_{\mathrm{NET}} = -\frac{kq}{x^2\left(1 + \dfrac{2r}{|x|}\right)}, \quad |x| \ge r \quad \text{(the diameter and outside).} \tag{9}$$

$$E_{\mathrm{NET}} = -\frac{kq}{3r^2}, \quad x = r\,. \tag{10}$$

We define the net charge equivalent q_{NET} at the diameter by specifying

$$q_{\mathrm{NET}} = -\frac{q}{3} = -e\,, \tag{11}$$

where e is elementary charge. Then (10) becomes $E_{\mathrm{NET}} = kq_{\mathrm{NET}} / r^2$ when $x = r$.

As x approaches infinity, (9) and (11) give $E_{\mathrm{NET}} = 3kq_{\mathrm{NET}} / x^2$ which is not in line with $E_{\mathrm{NET}} = kq_{\mathrm{NET}} / x^2$ expected from Coulomb's

Law. This gives a larger than expected field strength at large distances or a smaller than expected field strength at small distances from a charged particle, depending on the choice of where q_{NET} is set (at the diameter or infinity). Setting $q_{\mathrm{NET}} = -q$ to match Coulomb's Law at large x results in

$$E_{\mathrm{NET}} = \frac{kq_{\mathrm{NET}}}{x^2\left(1+\frac{2r}{|x|}\right)}, \quad |x| \geq r\,.$$

This field is less than the Coulomb's Law definition by 50% at 2 radii, 20% at 8 radii, and only 5% at 38 radii. Electrostatic interaction at large separation distances would show essentially no deviation from Coulomb's Law. This divergence would make charged particle short range interactions behave as if a separate attractive short-range force exists, compared to what Coulomb's Law specifies. If the particle were a point charge, this divergence would not occur.

Using (10) and (11), total electrostatic force is then

$$\mathrm{F_E} = q_{\mathrm{NET}}E_{\mathrm{NET}} = \frac{kq_{\mathrm{NET}}^2}{r^2} = \frac{kq^2}{9r^2}, \quad x = r\,. \tag{12}$$

By evaluating $|E|$ within radius r and total $|E|$ of the particle using (4) through (7), it can be shown that the fraction of total $|E|$, and therefore energy, within r is 1/3. Using $h\nu_g/3$ within a spherical volume of $4\pi r^3/3$ to represent the energy per volume, and using the standard EM equation $energy/vol = \varepsilon_0 E^2$ [5 p. 22], it can be shown that

$$q^2 = \frac{18\varepsilon_0 hc}{n}\,. \tag{13}$$

Then substituting for q^2 from (13) and one r from (1) into (12), we find

$$\mathrm{F_E} = \frac{h\nu_\mathrm{g}}{r}, \tag{14}$$

and total electrostatic force is repulsive for both negative and positive charge ring particles.

3.2. Gravitational force

The gravitational force between two half-masses of a particle, $h\nu_g/2c^2$, separated by a distance $2r$ is given by

$$\mathrm{F_G} = -\frac{Gm_1m_2}{(2r)^2} = -G\left(\frac{h\nu_\mathrm{g}}{4c^2r}\right)^2. \tag{15}$$

Comparing these electrostatic and gravitational forces for an electron, assuming classical CODATA electron radius [3]:

$$\mathrm{F_{Ee}} = 29.05350662\ \mathrm{N},$$

$$\text{and } \mathrm{F_{Ge}} = -4.359066922 \times 10^{-43}\ \mathrm{N}.$$

Gravitational force is insignificant in this model and will be ignored in further calculations.

3.3. Magnetic force

The standard magnetic force equation for a charge moving through a stationary field is $\mathbf{F}_\mathrm{B} = q\boldsymbol{u}_g \times \boldsymbol{B}$, where $\boldsymbol{u}_g \times \boldsymbol{B}$ is the cross product of group velocity vector $\boldsymbol{u}_\mathrm{g}$ and imposed magnetic field vector $\boldsymbol{B}$ [1]. For an EM wave in $n=1$ space, $\boldsymbol{B} = \mu_0\boldsymbol{H}$ where $H = (\varepsilon_\mathbf{0}/\mu_0)^{1/2}E$ [5 pp. 11, 21]. Since the wave has been wrapped onto a ring n times, the magnitude of both $\boldsymbol{E}$ and $\boldsymbol{H}$ are n times what they would be for an EM wave in $n=1$ space. Therefore $\mathbf{F}_\mathrm{B} = nq\boldsymbol{u}_g \times \boldsymbol{B}$. Using net charge and

field values appropriate for this model, we have $\mathbf{F}_{\mathrm{B}} = nq_{\mathrm{NET}}\boldsymbol{u}_g \times \boldsymbol{B}_{\mathrm{NET}}$. To a stationary observer, relative group wave motion between opposite sides of the ring is at velocity $2u_g = 2c/n$. Using that relative interaction velocity and the standard equation $c^2 = (\varepsilon_0\mu_0)^{-1}$ [5 p. 14] gives

$$\mathrm{F_B} = -2q_{\mathrm{NET}}E_{\mathrm{NET}}. \tag{16}$$

The direction of $\mathbf{F_B}$ is inward from the diameter to the center of the particle for both negative and positive charge models. Performing the same substitutions used in reducing the equation for $\mathbf{F}_{\mathrm{E}}$, we have

$$\mathrm{F_B} = -\frac{2h\nu_{\mathrm{g}}}{r}. \tag{17}$$

3.4. Combined forces

When we combine the always repulsive electrostatic and always attractive magnetic forces from (14) and (17), a net attractive force remains which is equal to $-h\nu_g/r$. This is equal to what the magnetic force would be for a static magnetic field and is the centripetal force that keeps the wave on a closed path around the ring.

4. Electron charge and refractive index

Solving (11) for q and substituting into (13) gives the net ring charge q_{NET}.

$$q_{\mathrm{NET}} = \pm\left(\frac{2\varepsilon_0 hc}{n}\right)^{1/2}, \quad n\text{=refractive index.} \tag{18}$$

Both this particle ring and its antiparticle twin have the same charge with opposite signs. Comparing this formula to the formula

derived for e from the fine structure constant equation $\alpha = 2\pi ke^2/hc$ [5 p. 186] indicates that for the electron,

$$n_e = \alpha^{-1} = 137.0359991 \tag{19}$$

where α is the fine structure constant. Since refractive index is a function of ε, we can generalize to say that the net charge of a particle with this theory is more properly shown as

$$q_{NET} = \pm\left(\frac{2\varepsilon hc}{n}\right)^{1/2}, \text{ where } \varepsilon/n = \varepsilon_0\alpha . \tag{20}$$

This form of the equation allows the net point equivalent charge of a proton to equal (with opposite sign) the charge of an electron, as long as the ratio $\varepsilon/n_p = \varepsilon_0\alpha$.

5. Spin and Bohr stability

The Bohr stability test (spin $P_s = mass * velocity * radius =$ an integer multiple of $h/2\pi$) can be extended from the atomic level to the particle level of this theory by using phase velocity. In the context of this theory, the de Broglie relation $\lambda = h/mu$ used in the Bohr hydrogen model [5 p. 184] would refer to the phase wavelength and phase velocity of a photon. Using $m = h\nu_g c^{-2}$ with (1) and (3), we find

$$P_s = mu_\phi r = \frac{h}{2\pi}, \tag{21}$$

and the test is satisfied. The quantization of internal spin is satisfied by the phase wave, not the group wave. When in a bound state or external field, there is nothing in this theory to prevent the electron's spin from being space quantized to its then accepted value $3^{1/2}h/4\pi$.

6. Absorption wavelength and proton refractive index

The author used CODATA mass energy values for the electron and proton [3] to derive their equivalent wavelength and frequency, using the relation $m_0 c^2 = h\nu_g$ where m_0 is rest mass. Using the corresponding pair production wavelengths, $n_e = 1/\alpha$, and several estimates of n_p, the author determined that the following relationships appear to exist.

$$\lambda_1 = 1.793956528\text{x}10^{-15}\ \text{m}, \tag{22}$$

$$\lambda_1 = \frac{2r_e}{\pi}, \tag{23}$$

$$\lambda_1 = \frac{2\pi r_p}{n_p}, \tag{24}$$

$$\frac{m_p}{m_e} = \frac{\pi^2 n_e}{n_p^2}, \tag{25}$$

$$n_p = 0.858248026. \tag{26}$$

This value of n_p was found via several analyses that led successively closer to the value shown, while at the same time λ_1 was being researched. Equations (23 - 25) brought both analyses together and set the values of λ_1 and n_p shown. The energy of a photon with wavelength λ_1 is 691.1214909 MeV.

7. Radii of the electron and proton

Solving (1) for r gives a theoretical circular radius. Elliptic minor and major axes are found by applying the appropriate power factor. For the electron,

$$r_e = 2.817940325\text{x}10^{-15}\ \text{m}, \text{ the classical electron radius,} \quad (27)$$

$$r_{emin} = \frac{\sqrt{2}}{2} r_e = 1.992584713\text{x}10^{-15}\ \text{m}, \text{ minor axis,} \quad (28)$$

$$r_{emaj} = \frac{2}{\sqrt{2}} r_e = 3.985169426\text{x}10^{-15}\ \text{m}, \text{ major axis,} \quad (29)$$

$$r_{erms} = r_{emin} + \frac{\sqrt{2}}{2}\left(r_{emaj} - r_{emin}\right) = 3.401554876\text{x}10^{-15}\ \text{m}. \quad (30)$$

For the proton,

$$r_p = 2.450444438\text{x}10^{-16}\ \text{m}, \quad (31)$$

$$r_{pmin} = \frac{\sqrt{2}}{2} r_p = 1.732725879\text{x}10^{-16}\ \text{m}, \text{ minor axis,} \quad (32)$$

$$r_{pmaj} = \frac{2}{\sqrt{2}} r_p = 3.465451758\text{x}10^{-16}\ \text{m}, \text{ major axis,} \quad (33)$$

$$r_{prms} = r_{pmin} + \frac{\sqrt{2}}{2}\left(r_{pmaj} - r_{pmin}\right) = 2.957948098\text{x}10^{-16}\ \text{m}. \quad (34)$$

This calculated proton rms radius differs significantly from CODATA's $R_p = 8.750\text{x}10^{-16}$ m derived from electron scattering experiments [3]. The author believes that an inherent assumption in the analysis of electron scattering may cause the discrepancy, and will

demonstrate how the CODATA value for R_p could include a large component related to the electron's elliptical shape.

An elliptical electron at closest approach to an elliptical proton in a scattering experiment will exhibit a varying distance between centers depending on ellipse orientations. We can calculate the experimental rms radius for a proton reported in such an experiment, assuming that the experimenter believes the electron is either circular in cross-section and the electron's diameter is its classical value, or the electron is a point particle but its classical diameter is assumed in calculations via use of, for instance, the Bohr radius, fine structure constant divided by electron mass, Rydberg constant, or Hartree energy.

Distances between centers at closest approach, assuming no overlap of elliptical perimeters or shape deformation are

$$d_{\min} = r_{\text{emin}} + r_{\text{pmin}}, \tag{35}$$

$$d_{\max} = r_{\text{emaj}} + r_{\text{pmaj}}. \tag{36}$$

The expected value to be reported for proton rms radius in such an experiment is then

$$\begin{aligned} \textit{Reported } R_{\text{pexprms}} &= d_{\min} + \frac{\sqrt{2}}{2}\left(d_{\max} - \mathrm{d}_{\min}\right) - r_{\mathrm{e}} \\ &= 8.794650244\text{x}10^{-16}\ \text{m} \\ &= 1.005102885\ R_{\mathrm{p}}. \end{aligned} \tag{37}$$

This theoretical *Reported* R_{pexprms} matches CODATA's R_p to within about 0.5%, while the standard uncertainty of R_p is nearly 0.8%. This qualifies as complete agreement.

Also significant is the range of reported radii that this theory predicts. By assuming the electron's orientation is random and the

proton's orientation is fixed at minimum or maximum interaction radius due to the nature of the scattering target, we can calculate the range of values that might be reported if classical electron radius is assumed in the experiment. The following range of values is found.

$$7.569197454\text{x}10^{-16}\,\text{m} \le \textit{Reported}\ R_{\text{pexprms}} \le 9.302249409\text{x}10^{-16}\ \text{m}\ . \quad (38)$$

This range should include the results of most scattering experiments that assume directly or indirectly a circular electron cross-section of classical radius.

8. Magnetic moment

Magnetic moment is calculated in the classical way $(\text{charge} * \text{area}/\text{period of rotation})$ except for the addition of two adjustments. First, group and phase waves are treated as equally capable of generating magnetic moments. Second, a precession of the ellipse is proposed because the group wavelength defined by the particle's energy is not an integer multiple of $2\pi r$ (or alternatively, refractive index n is not an integer). That precession adds an additional component to total magnetic moment.

Since n is not an integer for the electron or proton, the endpoint of group wavelength $2\pi rn$ does not correspond to the beginning location on the ring as seen by an outside stationary observer. The author proposes that a non-integer index of refraction, instead of unbalancing these rings, causes precession on the order of $(2\pi n)^{-1}$ fraction of one turn per turn. When $2\pi n$ trips of the wave around the perimeter have been completed, the ellipse has rotated one complete revolution.

The area of the ellipse is the same as the area of a circle of radius r. Group and phase wave contributions differ only in their velocities c/n and nc, affecting their periods. Period for the group component

is $2\pi rn/c$ and for the phase component $2\pi r/nc$. Total magnetic moment equals group μ plus phase μ, where each has a similar equation of the form

$$\text{group or phase } \mu = (1 + \text{precession factor}) * \text{charge} * \text{area/period}.$$

The total magnetic moment for one of these particles is then

$$\mu = \left(1 + \frac{1}{2\pi n}\right)\frac{ecr}{2}\left(n + \frac{1}{n}\right). \quad (39)$$

For the electron,

$$\mu_e = -9.285274825\text{x}10^{-24}\ \text{JT}^{-1} = 1.000055005\ \mu_e\ \text{CODATA}. \quad (40)$$

And for the proton,

$$\mu_P = 1.411596332\text{x}10^{-26}\ \text{JT}^{-1} = 1.000701558\ \mu_p\ \text{CODATA}. \quad (41)$$

Their antiparticles have the same values with reversed signs. These results represent very good fit between this basic theory and CODATA experimental values [3].

An even better fit for μ_e is possible by leaving out its group component. When that is done, $\mu_e = 1.000001746\ \mu_e$ CODATA, a reduction of about 97% in remaining anomaly. Then the remaining electron anomaly is only about 1.64 times the remaining proton anomaly. These considerations imply a real possibility that CODATA's μ_e does not include the group component, which is $n_e{}^2$, or about 18779, times weaker than the phase component and is associated with a period 18779 times greater. The proton's ratio of group/phase magnetic moment is about 1.36 and the CODATA value appears to include both components, from this theory's perspective.

9. Tests of the theory

The lack of an apparent electron internal structure in experimental evidence may be due to assumptions inherent in the analysis of data. A thorough modeling of expected interactions in electron-electron and electron-photon scattering, using the proposed model as a basis and relativistic electromagnetic and optical interactions, needs to be performed to see if theoretical scattering would then show the same results as experimental.

The specified divergence from Coulomb's Law at small separation distances for charged particles should be testable via re-analysis of a variety of experimental results. Direct comparison can also be made to current theories of short-range attractive forces affecting charged particles.

Refraction in this model is provided by an EM field whose Poynting vector opposes the Poynting vector of a passing EM wave. Such refraction should be testable through the use of an interferometer where one path proceeds through crossed electric and magnetic fields with a Poynting vector opposite the direction of passage of photons. EM field strengths might have to be considerable to generate an index of refraction large enough to observe, and both paths should be through vacuum. Since refractive index in a physical substance is normally proportional to the energy of the photon passing through, the same is expected in this test and relatively high photon energies might make the test more sensitive.

Experiments might be possible to detect and measure the electron's group magnetic moment, separate from its phase magnetic moment, as identified by this theory. If a separate group component does appear in testing, the theory would be supported.

This theory's accuracy in calculating the particle properties begs for experimental confirmation of anomalous dispersion at a specific

wavelength. It is not clear if an experimental test is straightforward, since it involves EM energy and no physical substance and may be specific to the EM ring particle structure. If the hypothesized anomalous dispersion applies to all photons, then photons of one wavelength λ_1 should be impossible to generate and detect since the λ_1 quantum would have infinite extent (because group and phase wavelengths would always be equal). Refraction of photons with wavelengths slightly larger and smaller than λ_1 would show anomalous behavior in a test that sends them through an EM field of sufficient strength with an opposing Poynting vector. An alternative explanation for the effects attributed to anomalous dispersion might also be found.

References

[1] W. Hauser, *Introduction to the Principles of Mechanics*, Addison-Wesley. (1966) 173.

[2] F.A. Jenkins and H.E. White, *Fundamentals of Optics*, McGraw-Hill/Maple. (1957)

[3] P.J. Mohr and B.N. Taylor, "CODATA recommended values of the fundamental physical constants: 2002", *Rev. Mod. Phys.* 77 (2005) 63-66.

[4] J.R. Reitz and F.J. Milford, *Foundations of Electromagnetic Theory*, Addison-Wesley. (1967) 339.

[5] R.T. Weidner and R.L. Sells, *Elementary Modern Physics*, Allyn and Bacon. (1966)